J Mol Model (2013) 19:779–792
DOI 10.1007/s00894-012-1604-z

ORIGINAL PAPER

Computational investigation of the key factors affecting the second stage activation mechanisms of domain II m-calpain

Gaurav Bhatti · Lakshmi Jayanthi · Pamela VandeVord · Yeshitila Gebremichael

Received: 8 February 2012 / Accepted: 21 September 2012 / Published online: 10 October 2012

Abstract The unique conformation of the active site in calpains along with the implication of their role in several diseases has prompted widespread research interest in the scientific community. Structural studies devoted to m- and μ-calpains have proposed a two-stage calcium-dependent activation mechanism for calpains. In this work, we performed conventional and targeted molecular dynamics simulations to investigate global and local changes in the structure of the protease core of m-calpain upon calcium binding. Simulations were performed on the protease core of calcium free (pdbid: 1kfu) and calcium bound (pdbid: 3df0) m-calpain with and without the presence of calcium ions. Our results indicate that the inactive, open conformation of the protease core does not transform into the active, closed conformation simply upon removal of constraints from the neighbor domains. The role of other factors, including calcium binding and the subsequent formation of an Arg94–Glu305 interdomain salt bridge and the change in the orientation of Trp288 side chain, in the activation of the protease core is elicited.

Keywords m-calpain · Calcium dependent activation

G. Bhatti · L. Jayanthi · Y. Gebremichael (✉)
Department of Biomedical Engineering, Wayne State University,
818 W. Hancock St.,
Detroit, MI 48201, USA
e-mail: yeshig@wayne.edu

P. VandeVord
School of Biomedical Engineering and Sciences, Virginia Tech,
Blacksburg, VA, USA

Introduction

Calpains (EC 3.4.22.52, EC 3.4.22.53) are a family of calcium-dependent, non-lysosomal cysteine proteases found in most organisms, ranging from single cell eukaryotes to mammals. They are important components of many cellular processes, and feature in numerous pathologies. Calpains are involved in an array of cellular processes such as cytoskeletal remodeling, cell cycle regulation, apoptosis, and motility [1–6]. In the brain, calpains have been implicated in a variety of physiological functions such as differentiation of neurons [7], neurite outgrowth [8], and synaptic remodeling [9]. On the other hand, altered calpain activities are associated with many human diseases. In particular, they are implicated in a number of neurological disorders like Alzheimer's, Parkinson's, and Huntington's diseases, where activation of the enzyme is believed to be an early step in the cascade of events leading to neuronal death [10]. Calpains are also linked to the pathological consequences of traumatic axonal injury (TAI) [11, 12], also known as diffuse axonal injury (DAI) [13].

To date, more than a dozen isoforms of calpain, which can be classified as either ubiquitously expressed or tissue-specific, are known. Among the ubiquitously expressed calpains, the most extensively studied isoforms are calpains I and II, also known as μ- and m-calpains, respectively. These isoforms differ from each other in their in vitro Ca^{2+} sensitivity and are activated at the micromolar (μ-calpains) and millimolar (m-calpains) ranges of Ca^{2+} concentration [14]. Structurally, both μ- and m-calpains exist as heterodimers composed of two distinct subunits, referred to as the large (80 kDa) and the small (30 kDa) subunits. The present study addresses the key activation mechanisms of m-calpain.

Structurally, m-calpain heterodimer consists of four domains (DI–DIV) in the large subunit and two domains (DV, DVI) in the small subunit [15, 16]. Figure 1 shows the structure of human m-calpain. Domain DI of the large subunit is an α-helical N-terminal anchor of 19 residues that tethers DII to DVI, and is partially autolysed upon Ca^{2+} binding. Domain DII consists of two catalytic subdomains, DIIa and DIIb, that correspond to papain-like active-site domains. The remaining two domains of the large subunit correspond to DIII, which shares structural similarity with the C2 domain of phospholipase C, and a C-terminal calmodulin-like domain, DIV. The two domains of the small subunit correspond to an N-terminal glycine-rich domain, DV, and a C-terminal calmodulin-like domain, DVI. Both domains DIV and DVI each contain five sets of calcium binding EF hand motifs found in other calcium-binding proteins like calmodulin. These domains bind four calcium ions each while the extreme EF hands of both domains interact with each other to form the heterodimeric structure [17].

Domains DIIa and DIIb of the large subunit constitute an essential component of the enzyme corresponding to the protease core—the region where the active site is found. The active site consists of the catalytic triad formed by three amino acid residues (Cys105, His262, and Asn286) that function together for catalysis. Of these three residues, Cys105 is on DIIa, whereas His262 and Asn286 are on domain DIIb**.** Proper assembly of these three residues is critical for enzymatic activity. Consequently, the large subunit is considered to serve as the unit of enzymatic activity. In contrast, the small subunit is required for the proper folding of the large subunit and is considered as a regulatory subunit. In the event of calpain activation, the small subunit is believed to dissociate from the large subunit due to calpain autolysis, although a recent study rejected this notion [18].

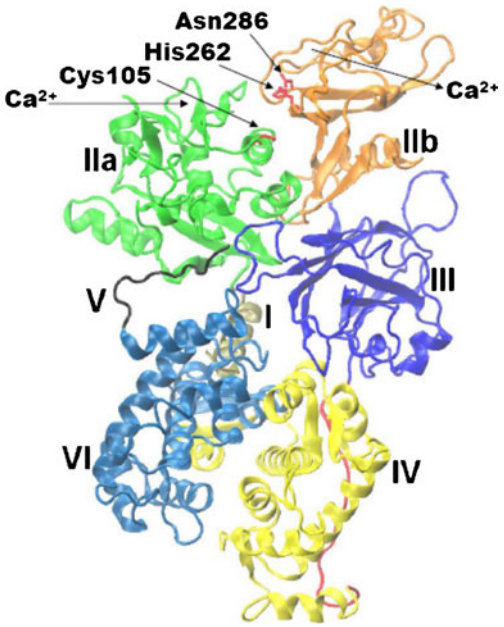

Fig. 1 Three-dimensional structure of calcium free m-calpain (pdbid: 1kfu). The figure was generated using visual molecular dynamics (VMD) [50]

In general, the activation of calpains is known to be distinct from those of classical proteases. In order to prevent premature degradation of substrates, all known cellular proteolytic enzymes are synthesized as zymogens or inactive precursors. The active sites of almost all zymogens are virtually indistinguishable when the proteins are converted into their related active protease. However, the inactive structure of calpains prior to Ca^{2+} binding is found to have a highly unusual conformation in which the active site corresponding to the catalytic triad is not assembled, which is unprecedented within the cysteine protease family [16]. This unique behavior of calpains along with their implied role in several diseases has prompted widespread research interest in the scientific community [6].

The Ca^{2+} requirements of the two ubiquitous isoforms of calpain are known to be high, approximately 3–50 μM and 400–800 μM for half maximal activity of μ-calpain and m-calpain, respectively [6], while the intracellular Ca^{2+} concentration is kept low (0.1–1 μM) [19]. This suggests that there must be other mechanisms that can lower the Ca^{2+} requirement of calpains to function under physiological conditions. Indeed, a number of factors such as autolysis, binding to phospholipids, membranes, or activator proteins were suggested to reduce the Ca^{2+} requirement to 1–5 μM for μ-calpains and 150 μM for m-calpains [6]. These values are still much higher than typical cytoplasmic Ca^{2+} concentrations, especially for m-calpain. As a result, the exact mechanism of calpain activation under normal intracellular Ca^{2+} concentration remains obscure.

Generally, calpain activation is known to involve many processes, including (1) local conformational changes of the three types of Ca^{2+}-binding site: the EF hands, the C2-like domain, and the protease core; (2) partial autocatalytic cleavage of the N-terminal domain DI, and perhaps subsequent dissociation of the small regulatory subunit DVI; and (3) rearrangements of the different Ca^{2+}-binding domains and their neighbors. The present study is concerned with understanding the local rearrangement of the protease core upon Ca^{2+}-binding. Clearly, Ca^{2+}-induced conformational changes and activation of calpains is a complex process involving the rearrangement of different domains. A comprehensive understanding of the activation process demands analyses involving the entire protein. However, resolving the factors governing the local structural reorganization of the catalytic domain (DII) allows for better understanding of Ca^{2+}-induced calpain activation.

In the past, many studies have analyzed the conformational changes of minicalpains (constructs consisting only of the protease core) of different isoforms [20–22]. Such studies

resolved the crystal structure of Ca^{2+}-bound minicalpains to predict the structural changes arising from Ca^{2+} binding. In these studies, the nature of Ca^{2+}-induced conformational transformations of the protease core was described by comparing the conformation of minicalpains with the protease core obtained from the Ca^{2+}-free m-calpain heterodimer. Ideally, it would be preferable if such comparisons were made based on Ca^{2+}-bound and Ca^{2+}-free protease cores both isolated from the same full-size m-calpain. This was not possible in the past due to the lack of Ca^{2+}-bound full-size m-calpain. Fortunately, recent success [23] in the structural determination of Ca^{2+}-bound m-calpain, along with the available Ca^{2+}-free m-calpain structure, now allows us to make this comparison. Especially, computer modeling can provide the means to explore the details of Ca^{2+}-induced calpain activation through insights into the dynamic local rearrangements of the protease core. Therefore, the goal of the present study was to map out Ca^{2+}-induced activation of the protease core (DII) by examining the conformational changes arising from key residues that are proposed to regulate calpain activation. To this end, we employed both equilibrium and targeted molecular dynamics (MD) simulations to assess the conformational changes under different conditions. The results of this analysis are presented below.

Materials and methods

We studied protease cores obtained from Ca^{2+}-bound and Ca^{2+}-free m-calpain heterodimers that serve as prototypes for studying the role of calcium and other factors in the realignment of the two sub domains (DIIa and DIIb) into a catalytically competent conformation. Different models of protease cores corresponding to the Ca^{2+}-bound, Ca^{2+}-free, point mutated, and other conditions were studied. The details of these models are described below and are also summarized in Table 1.

Model I: protease core of Ca^{2+}-free m-calpain

The coordinates for the initial structure of Ca^{2+}-free protease core were extracted from the crystal structure of the full-length (i.e., the structure containing all domains) Ca^{2+}free m-calpain heterodimer (pdbid: 1kfu) [15]. The protease core consists of 339 amino acid residues. The internal coordinate facility of CHARMM [36] was used to add the coordinates of the hydrogen atoms. The structure was solvated by using the TIP3P model of explicit water [37]. A cubic cell of 125 preequilibrated water molecules was replicated to form a cubic water box of 113.136 Å x 113.136 Å x 113.136 Å). All overlapping water molecules with their oxygen atoms within 2.4 Å of the ions and the heavy atoms of the proteins were deleted. The final system contained 46,000 molecules along with 339 protease core residues so that the total number of atoms of the whole system was 138,429. There was a distance of at least 13 Å on each side between the protein and the boundaries of the water box. The histidine residues in the protease core were protonated based on their distances from nearby donors or acceptors. The net charge of the protease core was −14 at pH 7. SOLVATE 1.0 [38] was used to neutralize and get the desired ionic strength for the system by placing potassium and chloride ions based on the Debye-Huckle distribution. The final ionic strength of the system was around ~112 mM. With this system, two independent simulations, 1kfunoca and 1kfunoca1, were carried out for durations of 21 ns and 19 ns, respectively.

Model II: protease core of Ca^{2+}-bound m-calpain

The crystal structure of full-length calcium bound m-calpain heterodimer (pdbid: 3df0) [23] was used to extract the coordinates of Ca^{2+}-bound protease core along with the calcium ions. This was used as the initial structure for the simulation of active protease core with a closed initial conformation. The modeling protocol for this system is the

Table 1 Initial structural properties of protease core in different models. Orientation I refers to Trp288 orientation, where the side chain of Trp288 is in the region in between the two sub domains, IIa and IIb (cf. Fig. 4a), and Orientation II refers to the Trp288 orientation where its side chain is rotated towards domain IIb (cf. Fig. 4b)

Model	PDB ID	Simulation ID	Ca^{2+} presence	Salt bridge	TRP288 orientation	E323A mutation
Model I	1KFU	1kfunoca1	Absent	Absent	Orientation I	No
Model I	1KFU	1kfunoca2	Absent	Absent	Orientation I	No
Model II	3DF0	3df0ca	Present	Present	Orientation II	No
Model II	3DF0	3df0ca1	Present	Present	Orientation II	No
Model II	3DF0	3df0ca2	Present	Present	Orientation II	No
Model III	3DF0	3df0noca1	Absent	Present	Orientation II	No
Model III	3DF0	3df0noca2	Absent	Present	Orientation II	No
Model IV	3DF0	3df0mut	Present	Present	Orientation II	Yes

same as Model I. There were a few differences in residues between this structure and the structure used to study the open conformation (pdbid: 1kfu) because of the difference in the genetic source (Rat for 3df0 and Human for 1kfu). However, most residues believed to be critical for the enzyme activity are highly conserved among different species. The number of ions needed to neutralize and achieve the desired ionic strength (~112 mM) was adjusted. The total number of atoms in the system was 138,342. For this system, three independent MD simulations, 3df0ca, 3df0ca1 and 3df0ca2, were carried out for durations of 28 ns, 24 ns and 24 ns, respectively.

Model III: Ca^{2+}-free closed conformation of the protease core

In order to assess conformational changes due to the removal of Ca^{2+} from the Ca^{2+}-bound m-calpain protease core, we removed calcium ions from the protease core of the full-length Ca^{2+}-bound m-calpain (pdbid: 3df0) to generate a model of Ca^{2+}-free closed protease core. Once again the same modeling protocol was used, except for different numbers of potassium and chloride ions to reach an ionic strength of ~112 mM. The total number of atoms in the system was 138,300. For this system, two independent simulations, 3df0noca1 and 3df0noca2, were carried out for a period of 23 ns each.

Model IV: point mutated (E323A) Ca^{2+}-bound protease core

The presence of a salt bridge between ARG94 and GLU323, which are located on the facing sides of the two subdomains (domains DIIa and DIIb) of the protease core, has been suggested as an important factor in establishing the closed conformation of calcium bound m-calpain. To study the effect of the Arg94–Glu323 double salt-bridge on the stability and conformation of the Ca^{2+}-bound closed protease core, we mutated Glu323 to Ala. This was done by replacing the coordinates of atoms in the residue Glu323 of the original PDB file with the atoms of an alanine residue. The rest of the model was built using the same procedure described above with minor changes in the number of counter ions added to reach an ionic strength of ~112 mM. The total number of atoms in the system was 138,369. One simulation, 3df0mut, of the system was performed for a duration of 19 ns.

Molecular dynamics simulations

NAMD 2.6 [39] with CHARMM22 force field parameters [40] was used to perform conventional MD simulations for all models. The models were prepared using CHARMM [36] and then the NAMD program [39] was used for the minimization, equilibration and production runs. The trajectories obtained from the production run were then analyzed using the CHARMM analysis facility [36]. Periodic boundary conditions were applied based on the cubic symmetry of the simulation box. The cut-off value was set at 12 Å for non-bonded interactions and with a switching function from 8 Å to 12 Å. The particle-mesh Ewald method [41] was employed to compute the long-range electrostatic interactions with tolerance set at 1.0e−6. Simulations were done with time step of 2 fs. The system was minimized and equilibrated in multiple stages using protocol similar to one followed for an actin system [42]. First, the system was minimized by using two alternating methods: (1) velocity quenching minimization (5,000 steps), (2) conjugated-gradient minimization (19,000 steps). During the minimization, constraints were applied on the Cα atoms to restrain them to their initial positions using harmonic potentials (100 kcal/mol per Å). Next, the system was heated to 310 K via velocity assigning at every 0.2 ps at a rate of 31 K/ps for 10 ps. Constraints were applied to the Cα atoms during the heating stage. The system was then allowed to equilibrate while the constraints on the Cα atoms were released gradually (100 kcal/mol per Å for 10,000 steps, 10 kcal/mol per Å for 15,000 steps, 1 kcal/mol per Å for 20,000 steps). For the last 25,000 steps of equilibration, constraints on the Cα atoms were released. MD simulations were then performed under constant NPT ensemble for durations ranging from 19 to 28 ns for different systems. Langevin thermostats (damping coefficient=0.5 ps^{-1}) were used to control the system temperature at 310 K. Langevin-piston barostat (piston period of 2 ps and a damping time of 2 ps) was used to control the system pressure at 1 atm.

Targeted MD simulations

Targeted MD has proven to be an efficient tool to study the conformational changes of different biomolecules [43–47]. The method applies a constraining force on a known initial structure to guide it to a desired target structure, by reducing the distance between the two known structures in a time-dependent manner. Mathematically, it is represented as

$$\sum (X_i(t) - X_{T_i})^2 - \rho(t)^2 = 0,$$

where $X_i(t)$ represents the position of atom i of the initial structure at time t and X_{T_i} is the position of atom i in the target structure. $\rho(t)$is the desired root mean square deviation (RMSD) between the two structures, and is decremented linearly with each time step. More details on the TMD simulation method can be found in the literature [44, 45]. In the present study, TMD simulations as implemented in CHARMM [36] were performed to assess changes in the side chain orientation of Trp288 as the protease core

transforms from a closed, active conformation (pdbid: 3df0) to the open, inactive conformations (pdbid: 1kfu). As reference structures for the initial closed conformation and for the target open conformations, we selected the equilibrated structures of the protease cores extracted from the crystal structure of the closed, active m-calpain heterodimer (pdbid: 3df0) and the open, inactive m-calpain heterodimer (pdbid: 1kfu), respectively. For the TMD study, three independent simulations were carried out, with a time step of 1 fs applied for the dynamics. The starting structures were minimized from their crystal structures by using the steepest descent method and multiple step equilibration protocols as described in the section on traditional MD simulations. The simulation was performed in an implicit solvent environment at an ionic concentration of 150 mM by using the generalized Born with simple smoothing functions (GBSW) implicit solvent model [48, 49] as implemented in CHARMM [36]. During the simulations, TMD forces were applied to the backbone of all atoms in the protease core. The side chains were kept free to adjust through the system dynamics. This allowed us to observe the free re-orientation of Trp288 side chains upon conformational transformation of the protease core from closed to open conformation. The initial value of ρ was found to be 5.8 Å, and was decremented linearly from 5.8 Å to 0.8 Å in steps of 0.000016 Å. The trajectories obtained from these simulations were analyzed visually using visual molecular dynamics (VMD) [50].

Results and discussion

m-Calpain consists of ten Ca^{2+}-binding sites throughout the heterodimer [23]. The presence of such a large number of Ca^{2+} binding sites, along with the autolysis of its domains, makes calpain activation a complex process. In the past, many structural data have been reported that have been useful in revealing the molecular mechanisms behind Ca^{2+} activation [15, 16, 24]. Among these, the crystal structure of Ca^{2+}-free m-calpain heterodimer [15, 16] has been instrumental in offering insights into the regulatory mechanism of calpains and the Ca^{2+}-induced switch between active and inactive forms. The critical observation from this structure is that the residues in the catalytic triad are not assembled, i.e., the catalytic Cys105-S in DIIa is ~10.5 Å away from His262-Nδ, i.e., too far to form competent catalytic triad [15, 16]. Based on this, it was concluded that Ca^{2+}-free calpains are in their open inactive forms, and Ca^{2+}-induced conformational changes must take place in order to assemble the catalytic triad and form an active protease in calpain [15, 16]. This was confirmed by the recent determination of the structure of the Ca^{2+}-bound m-calpain heterodimer (pdbid: 3df0) [23], which revealed Ca^{2+}-induced assembly of the catalytic triad into a catalytically competent closed conformation, i.e., the distance between Ser105-Oγ and His262-Nδ is reduced to 3.48 Å, similar to the Ca^{2+}-bound minicalpains [20, 21]. Note that, in the crystal structure of Ca^{2+}-bound m- calpain (pdbid: 3df0), Cys105 is mutated to Ser105 for crystallization and therefore catalytic distance is calculated between Ser105-Oγ and His262-Nδ.

Prior to the availability of the Ca^{2+}-bound m-calpain structure, Ca^{2+}-bound minicalpains and biochemical analyses were employed to investigate the molecular basis of Ca^{2+}-induced calpain activation [20–22]. On the basis of these latter studies, a two-stage mechanism involving the release of constraints imposed by domain interactions (first stage) followed by rearrangement of the active site cleft (second stage) was proposed [21]. In the second stage, a number of key residues considered to play a critical role in the switch between active and inactive conformations have been identified. Some of these include the double salt-bridge between the side chains of Arg94 and Glu323, the orientation of Trp106, which was suggested to occlude the active site cleft, and the orientation of Trp288, which acts as a wedge between the two sub domains of the protease core, affecting the assembly of the active site cleft [20, 21]. In this regard, the recent crystal structure of Ca^{2+}-bound m-calpain (pdbid: 3df0) has been instrumental in revealing the structural implications of these key residues [23]. However, many questions remain unanswered. These include: to what extent does the release of the constraints on DII allow the two lobes of the protease core to come together? What is the sole effect of Ca^{2+}-binding at the two lobes in causing local structural rearrangements that favor the establishment of the active conformation? Which of the suggested key residues is critical in regulating the second-stage activation mechanism? The present study attempted to address these issues as described below.

Study on conformational changes of the protease core using equilibrium MD simulation

To address the questions raised above, we carried out a number of independent MD simulations of the protease core, under both Ca^{2+}-bound and Ca^{2+}-free conditions. The latter was obtained (1) by extracting the protease core from the crystal structure of the open Ca^{2+}-free m-calpain (pdbid: 1kfu), and (2) by removing the Ca^{2+}-ions from the protease core obtained from the crystal structure of the Ca^{2+}-bound m-calpain (pdbid: 3df0). The effect of Trp288 reorientation along with salt-bridge mutation and calcium removal was studied by examining the distance between the active site residues as a function of equilibrated simulation times.

Effect of releasing neighboring domains constraints

In the past, several studies have proposed that the binding of calcium to calmodulin-like EF hands on domains IV and VI,

and possibly to the C2-like domain III, releases the constraints on the protease core, ultimately bringing together sub domains IIa and IIb into an active closed conformation [15, 16, 24]. This proposal can be tested computationally by examining changes in the distance between the catalytic residues when the neighboring domains constraining the protease core are released. Extracting the protease core from the full size m-calpain heterodimer and then fully equilibrating by running MD simulations allows us to assess the changes due to release of neighboring constraints. To this end, we measured the distance (hereafter referred to as catalytic distance) between the S atom and the N_δ atom of the catalytic Cys105 and His262 residues, respectively, of the isolated protease core. These residues are located on opposite lobes of the protease core, i.e., Cys105 is located on sub domain DIIa and His262 is on sub domain DIIb, and play a critical role in catalytic activity.

In the active closed conformation of cysteine proteases, the catalytic residues Cys105 and His262 form an ion pair in the assembled active site. In a common cysteine protease, papain, the distance between the S atom of Cys and N_δ atom of His is around 3.7 Å [25, 26]. At this distance, the His-N_δ atom coordinates with the hydrogen atom that is bonded to Cys-S, lowering the dissociation constant of S and increasing its negative charge, rendering it nucleophilic [25, 26]. Similarly, the separation between Cys105-S and His262-N_δ determines whether or not the protease core of m-calpain is active. In the crystal structure of Ca^{2+}-free m-calpain (pdbid: 1kfu), the catalytic distance is ~10.5 Å, i.e., too large for the cysteine and histidine residues to form an ion pair, thereby making the structure inactive [15–17, 24]. By contrast, the catalytic distance of the Ca^{2+}-bound m-calpain (pdbid: 3df0) in its closed active conformation is 3.48 Å, i.e., closer to the value seen in active cysteine proteases [25, 26]. (Note that in the Ca^{2+}-bound m-calpain, the catalytic Cys105 is mutated to Ser105 for crystallization, and the catalytic distance is between Ser105-Oγ and His262-Nδ.)

To assess changes arising from the release of neighboring domain constraints on the conformation of the active site cleft, we measured the distance between the S atom of Cys105 and the N_δ atom of His262 of the protease core obtained from the Ca^{2+}-free full-size m-calpain (pdbid: 1kfu). Figure 2a shows a plot of the catalytic distance, d, as function of time, t, for the simulation of Ca^{2+}-free m-calpain protease core (referred to as model I, see Methods section). The plot shows that the release of domain constraints reduces the distance between the active site residues in one of the independent simulations from 10.5 Å to an average value of 5.66 Å, whereas in another independent simulation, the catalytic distance rather increased from 10.5 Å to an average value of 16.16 Å towards the last 5 ns. Further, examination of data from the two independent simulations (i.e., 1kfunoca1 and 1kfunoca2) reveals that the increase in d was due not to the increase in the separation between the two sub domains, IIa and IIb, but rather to the re-orientation of the side chains of two catalytic residues, His262 and Cys105, away from each other. This can be confirmed by observing the inter-domain angle, Θ (to be discussed below), which shows a similar behavior for the two independent simulations (Fig. 3a). It is obvious from the two simulations that the mere release of constraints did not result in a closed conformation, i.e., neither did the catalytic distance, d, decrease to values observed in the active Ca^{2+}-bound m-calpain or papain, nor did the two sub domains move towards each other. This implies that the mere release of constraints from neighboring domains will not necessarily facilitate the folding of the enzyme to its closed conformation. The observed increase of the catalytic distance in one of the two simulations rather suggests the unstable behavior of the constraint-free protease core that is extracted from the Ca^{2+}-free heterodimer. As will be discussed below, other factors are observed to play essential roles in stabilizing the closed active conformation.

Effect of Ca^{2+} in stabilizing the active conformation

The analysis discussed above assesses the role of neighboring constraints in the absence of Ca^{2+}, in order to be able predict the isolated effect of the constraints. On the other hand, the effect of Ca^{2+} on the organization of the active site cleft can be determined by examining MD simulations of the protease core in both the presence and absence of Ca^{2+}. Such analysis is motivated by many past studies that employed computational methods to predict the structural preference of proteins upon Ca^{2+} binding [27–31]. For example, Shesham et al. [27] employed MD simulations to study Ca^{2+}-induced conformational changes of annexin I. Li et al. [28] performed MD simulations to investigate the Ca^{2+}-induced changes of recoverin, whereas Komeiji et al. [29], Shepherd et al. [30], and Project et al. [31] all studied Ca^{2+}-dependent conformational changes and the effect of Ca^{2+} removal on calmodulin protein, again by using MD simulations. In a similar manner, we performed MD simulations of Ca^{2+}-bound (model II) and Ca^{2+}-free (model III) m-calpain protease cores to assess the role of Ca^{2+} in maintaining the closed active conformation. Both Ca^{2+}-bound (model II) and Ca^{2+}-free (model III) protease cores were obtained from the Ca^{2+}-bound active full-size m-calpain (pdbid:3df0); the Ca^{2+}-free structure (model III) is prepared by simply removing Ca^{2+} from the protease core. Note that, although both models I and III are Ca^{2+}-free protease cores of m-calpain, they have different initial conformations. In model I, the protease core was extracted from the crystal structure of the Ca^{2+}-free m-calpain heterodimer (pdbid: 1kfu) and has an open initial structure. In model III, the protease core is extracted from the crystal structure of Ca^{2+}-

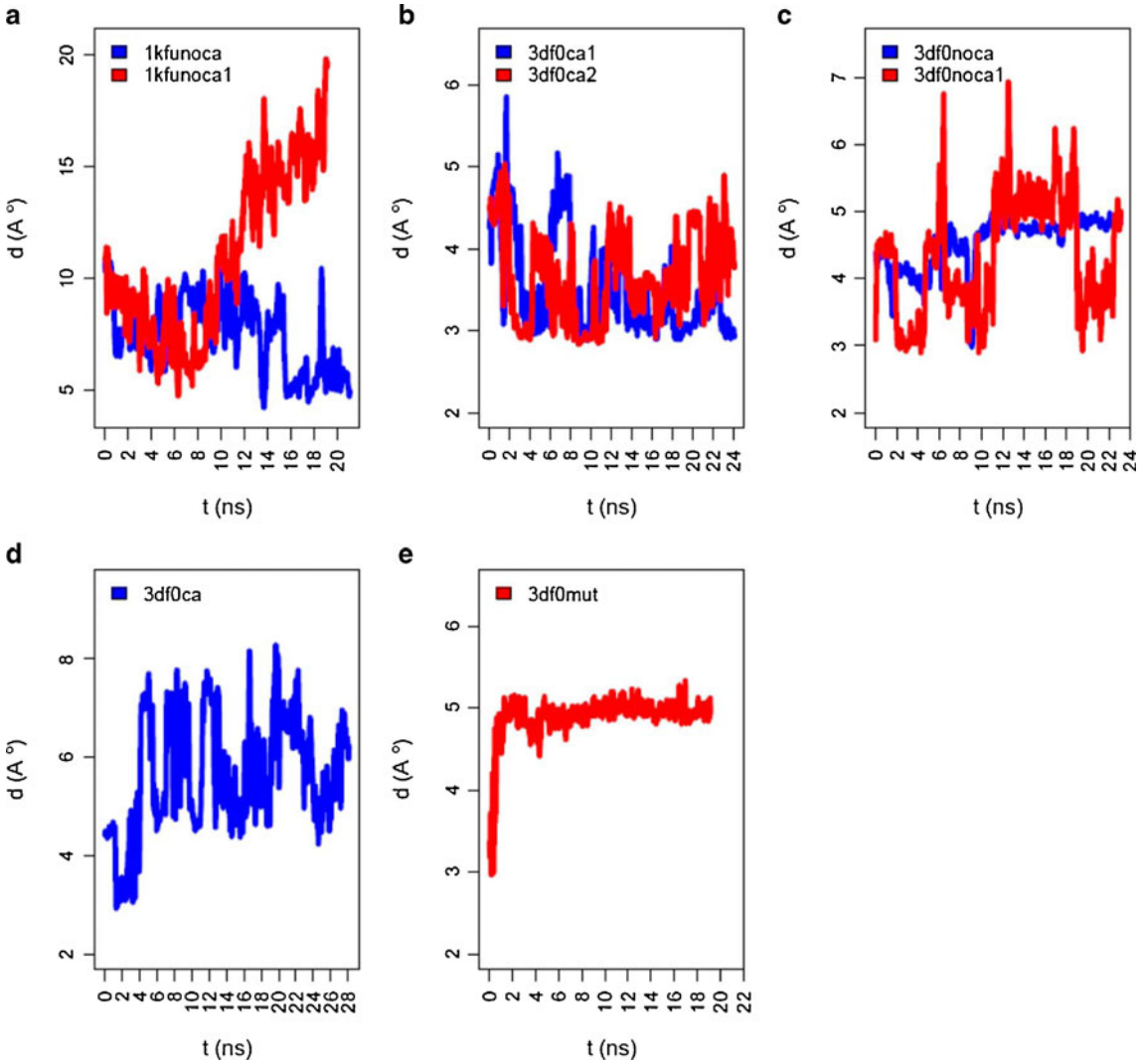

Fig. 2 Plots of the catalytic distance, *d* (Å), as a function of time, *t* (ns) for different models. **a** Two independent simulations of model I (Ca^{2+}-free protease core extracted from Ca^{2+}-free m-calpain heterodimer, pdbid: 1kfu). **b** Two independent simulations of model II (Ca^{2+}-bound protease core extracted from Ca^{2+}-bound m-calpain heterodimer, pdbid: 3df0). **c** Two independent simulations of model III (Ca^{2+}-free protease core extracted from Ca^{2+}-bound m-calpain heterodimer, pdbid: 3df0). **d** A model with a re-oriented Trp288 (rare event case of model II), and **e** model IV (Ca^{2+}-bound protease core of Ca^{2+}-bound m-calpain heterodimer with GLU323ALA mutation, pdbid: 3df0). Note that running averages were applied to smooth the plots. Note also that the plot in **d** corresponds to the system in which a transition from the closed to open conformation was observed in terms of *d*, and inter domain angle, Θ. The figure was generated using R [51]

bound m- calpain heterodimer (pdbid: 3df0) and has a closed initial conformation.

The catalytic distance for both models was measured to assess the changes in the active site cleft arising from the removal of Ca^{2+}. Figures 2b,c depicts the plot of the catalytic distance, *d*, as function of time, *t*, for the Ca^{2+}-bound (model II) and Ca^{2+}-free (model III) protease cores, respectively. As shown in the figure, the Ca^{2+}-bound structure exhibits a stable active conformation in which the catalytic distance remains within a range expected for closed conformation. In these simulations, the catalytic distance, *d*, remains close to the initial value of d=3.48 Å, with average values for the last 5 ns being 3.212 Å (3df0ca1) and 3.99 Å (3df0ca2) for two independent simulations of Ca^{2+}-bound m-calpain protease core (model II).

In contrast, the Ca^{2+}-free structure (model III) is observed to swing between active and inactive conformations in one of the independent simulations (Fig. 2c, 3df0noca1), where the catalytic distance swings between, on average, d= 3.522 Å (active) and d=4.97 Å (inactive) conformations. In another independent simulation (Figs. 2c, 3df0noca), the Ca^{2+}-free structure remains mostly in the inactive conformation with the average value of *d* being 4.54 Å over 23 ns. Using an approximate cut-off distance of 4 Å (based on references [32–34]) to distinguish between the catalytically competent and catalytically disrupted conformations, these

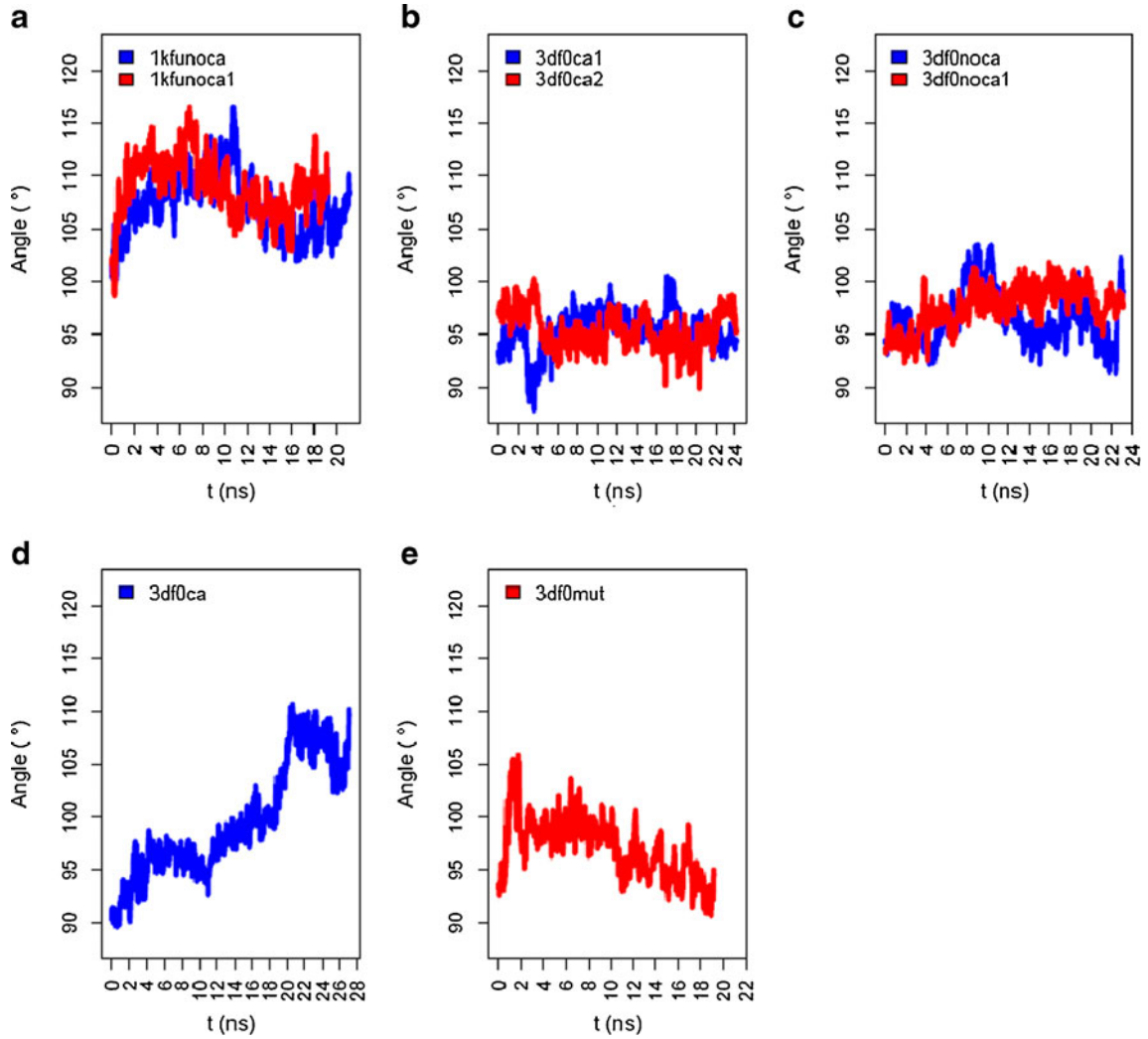

Fig. 3 Plots of inter domain angle, Θ (°), as a function of simulation time, t(ns), for different models. **a** Two independent simulations of model I (Ca^{2+}-free protease core extracted from Ca^{2+}-free m-calpain heterodimer, pdbid: 1kfu). **b** Two independent simulations of model II (Ca^{2+}-bound protease core extracted from Ca^{2+}-bound m-calpain heterodimer, pdbid: 3df0). **c** Two independent simulations of model III (Ca^{2+}-free protease core extracted from Ca^{2+}-bound m-calpain heterodimer, pdbid: 3df0). **d** A model with a re-oriented Trp288 (rare event case of model II), and **e** model IV (Ca^{2+}-bound protease core of Ca^{2+}-bound m-calpain heterodimer with GLU323ALA mutation, pdbid: 3df0). Note that running averages were applied to smooth the plots. Note also that the plot in **d** corresponds to the system in which a transition from the closed to open conformation was observed in terms of the catalytic distance, *d*, and inter domain angle, Θ. The figure was generated by using R [51]

data suggest that Ca^{2+} makes a significant contribution to stabilizing the closed active conformation. However, as will be shown below, further additional factors play a role in maintaining the closed active conformation.

Role of salt-bridges in maintaining the closed conformation

In the proposed mechanism for the second stage activation of m- calpain, the double salt-bridge between Arg94 (subdomain DIIa) and Glu323 (subdomain DIIb) is considered critical since it is absent in the Ca^{2+}-free structure [21]. To test the contribution of the Arg94-Glu323 salt-bridge in maintaining the closed conformation and to assess the conformational changes arising from salt-bridge disruption, we performed another equilibrium MD simulation (model IV) with a Glu323Ala mutation to abolish the salt-bridge interaction. This mutation is analogous to the mutagenesis experiment that resulted in severely impaired enzyme activity of μ-minicalpain at low Ca^{2+} concentration [35]. The mutated protease core allows us to predict the rearrangement of the active site cleft arising from salt-bridge disruption, revealing the importance of the salt-bridge in active site formation. We use catalytic distance as a measure of proteolytically competent conformation in the Glu323Ala mutated system to assert the role of the Arg94-Glu323 salt-bridge.

Figure 2e shows a plot of the catalytic distance, *d*, as a function of time for the mutated model (model IV). In our simulation, we used the protease core of Ca^{2+}-bound m-calpain heterodimer (pdbid: 3df0) for the mutation, and the Ca^{2+} ions were retained in the mutated protease core. Interestingly, despite the presence of Ca^{2+}, the Glu323Ala mutation resulted in an average catalytic distance of d=4.9 Å. In this case, *d* increased from 3.43 Å to 5 Å within the first 3 ns and then settles at around 5 Å for the remaining simulation period (i.e., ≈16 ns). Comparison with a similar Ca^{2+}-bound protease core (model II) reveals that the presence of a salt-bridge plays a significant role in maintaining the closed, catalytically competent, catalytic conformation.

Role of the side chain orientation of Trp288 in the transformation of DII from inactive to active conformation

Among the key residues suggested to be critical in the activation of calpains, reorientation of the Trp288 side chain has been considered as important in the closed to open conformational transformation [7, 21]. In the Ca^{2+}-free inactive conformation, the indole ring of Trp288 is found to be oriented in between the sub domains DIIa and DIIb, acting as a wedge between the two (Fig. 4a shows Trp288 orientation in the crystal structure of Ca^{2+}-free m-calpain, pdbid: 1kfu). In the Ca^{2+}-bound active conformation, the indole ring is oriented away from the catalytic cleft (Fig. 4b, taken from the crystal structure of Ca^{2+}-bound m-calpain, pdbid: 3df0). This rotation of the tryptophan side chain away from the cleft has been ascribed as a precondition for the assembly of a proteolytically competent catalytic triad [15, 21]. In this regard, Moldoveanu et al. reported that the binding of calcium ions to the subdomains DIIa and DIIb results in the rotation of the indole ring of Trp288 from its wedge-like position into a Ca^{2+}-induced hydrophobic pocket that fully buries one of its sides [21].

As expected, visual inspection of the indole ring of Trp288 in the Ca^{2+}-free protease core (model I) reveals that the orientation of the side chain remains in between the two subunits at all simulation times. In contrast to model I, the side chain of Trp288 in the simulations of the protease cores extracted from Ca^{2+}-bound m-calpain heterodimer (model II and model III) is found to be rotated away from in between the two sub domains into the hydrophobic pocket consisting of residues V253, V259 and V291. Recall that model II and III are Ca^{2+}-bond and Ca^{2+}-free protease cores, respectively, that were originally extracted from the Ca^{2+}-bound heterodimer (pdbid: 3df0). Irrespective of Ca^{2+}-binding, the Trp288 side chains in the two systems were found to remain close to the hydrophobic pocket at all simulation times. A similar behavior was observed in the mutation simulation (Ca^{2+}-bound protease core with Glu323Ala mutation, model IV) i.e., the side chain of Trp288 remained in the orientation belonging to the Ca^{2+}-bound heterodimer structures that they were extracted from. However, in one independent simulation of the Ca^{2+}-bound protease core (model II), we found a situation in which the indole ring of Trp288 moved away from the expected hydrophobic pocket into the region in between the two sub domains (Fig. 4c,d). In the same simulation, the catalytic site was found disrupted, with the catalytic distance changing from about 3.45 Å to 6.69 Å (Fig. 2d). This motivated the targeted MD simulation (discussed below) study that overcomes the potential barrier in the free orientation of Trp288 side chain upon transformation from closed to open conformation.

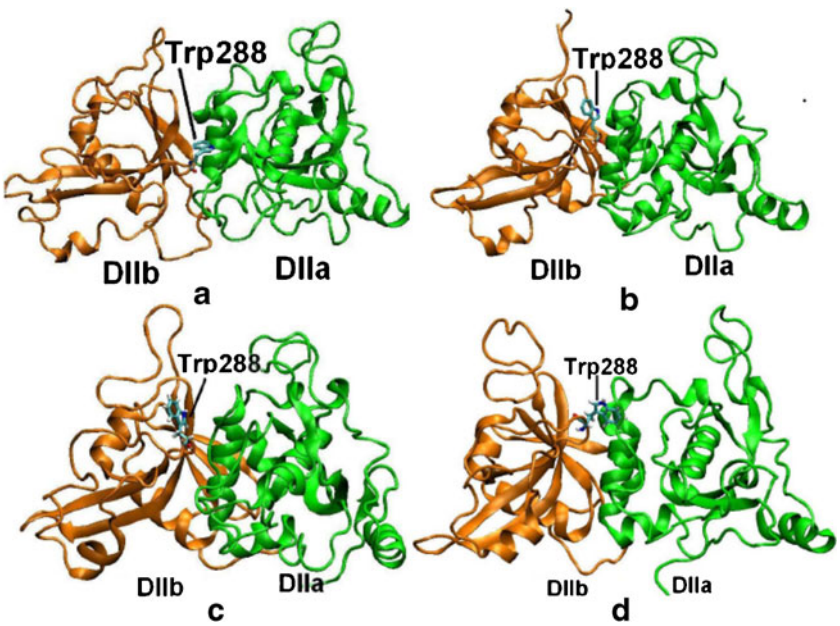

Fig. 4 Side-chain orientation of Trp288 in **a** the protease core of calcium free m-calpain heterodimer (pdbid: 1kfu), **b** the protease core of calcium bound m- calpain heterodimer (pdbid: 3df0), **c** the structure of the protease core that underwent Trp288 re-orientation when observed before the rotation took place (see the same system in Fig. 1d), and **d** the protease core described in **c** after the Trp288 side chain rotation took place. Note that **a** and **b** belong to the structures obtained from the protein data bank, whereas **c** and **d** are the snapshots taken from MD simulations. The figures were generated using VMD [50]

Before examining the TMD data, it is worth discussing the extent of closed or openness of the two lobes under different conditions, which was assessed by measuring the inter-domain angle, Θ. We define Θ as the angle between the vectors joining the Cα atom of Glu205 and the center of masses of domains IIa and IIb. The glutamate residue, Glu205 was chosen because its location was close to the loop joining the two sub domains and it has low RMSF values in all systems studied (data not shown). As a reference, the inter-domain angle for the original structure, i.e., the crystal structure of Ca^{2+}-free open protease core (pdbid: 1kfu) is 104.77°. A similar value was found for Ca^{2+}-bound protease core (pdbid: 3df0): 92.17°.

The inter-domain angle, Θ, was calculated for different simulation conditions, and Fig. 3 shows the plot of Θ as a function of time, *t*, for these simulations. In both simulations of Ca^{2+}-free protease core extracted from Ca^{2+}-free m-capain heterodimer (model I), 1kfunoca and 1kfunoca1, Θ changed from an initial value of 104.77° to an average value of 105.31° and 107.81°, respectively, for the last 5 ns (Fig. 3a). Comparison of Fig. 3a with Fig. 2a indicates that the sharp increase in the catalytic distance *d* of the 1kfunoca1 model as opposed to the decrease observed in the 1kfunoca model can be explained in terms of the orientation of the side chains as opposed to the inter domain separations.

In two out of three independent simulations of model II (Ca^{2+}-bound protease core extracted from Ca^{2+}-bound m-calpain heterodimer), i.e., 3df0ca1 and 3df0ca2, Θ changed from an initial value of 92.17° to an average value of 94.74° (3df0ca1) and 95.42° (3df0ca2), respectively, in the last 5 ns (cf. Fig. 3b). The corresponding values for the two simulations (3df0noca and 3df0noca1) of model III (Ca^{2+}-free protease core extracted from Ca^{2+}-bound m-calpain heterodimer) are 96.215° and 98.40°, respectively (cf. Fig. 3d). Thus we see that the originally Ca^{2+}-bound protease cores tend to retain their closed conformations, even after the removal of Ca^{2+} in the case of model III. In the simulation of the salt-bridge mutated structure (model IV, 3df0mut), the inter domain angle, Θ, increased initially and then decreased (Fig. 3e). Although Θ showed a tendency to decrease, the catalytic distance, *d*, increased in this model (Fig. 3e). Using *d* as a metric for the likelihood of forming active conformation, this observation suggests the effect of the absence of the Arg94-Glu323 salt-bridge in destabilizing the active conformation.

The third simulation of Ca^{2+}-bound structure (model II, 3df0ca) is one of the equilibrium MD simulations that exhibited Trp288 side chain rotation. Here, we clearly noticed a transition from closed to open conformation, i.e., Θ increased from 92.17° at the beginning of the simulation to an average (last 5 ns) of 106.29° (Fig. 3d). Figure 5a,b shows snapshots of the protease core near the beginning and end of simulations, respectively. The time evolution of the inter-domain angle as the protease core transforms from closed to open conformations is depicted in Figs. 3d and 5c. The results presented in these figures are interesting since such a significant transformation from closed to open conformation (in terms of Θ) was observed only in the simulation where we also witnessed the event of Trp288 indole ring reorientation. This data suggests that the change in the orientation of Trp288 is associated with transformation of the protease core from active to inactive conformation and vice versa. The transition of the Trp288 side chain from its closed to open conformation was explored further using the targeted MD simulation method.

Targeted MD simulations

The conventional MD simulations described so far provided valuable information on the role of major factors such as calcium binding, Arg94-Glu323 double salt bridge and side chain orientation of Trp288 in maintaining the open and closed conformations of the protease core of m-calpain. However, it is often challenging to reproduce large-scale conformational changes as seen in Trp288 re-orientation by using conventional MD simulations. Therefore, we performed three independent targeted molecular dynamics (TMD) simulations to accelerate the transition of the protease core from closed to open conformation. We wanted to examine if Trp288 undergoes re-orientation as the conformation of the protease core transforms from closed, active conformation to open, inactive conformation. As mentioned in the previous section, in the open conformation, the side chain of Trp288 is oriented in between the two sub domains, thereby acting as a steric barrier to their fusion. Upon calcium binding, the side chain of Trp288 moves into a hydrophobic pocket located at the sub domain DIIb thus clearing the way for the sub domains to move towards each other. In our TMD simulations, we observe that, as the protease core of calcium bound m-calpain (closed conformation) approaches the conformation of the protease core of calcium free m-calpain (open conformation), the side chain of Trp288 moves away from the hydrophobic pocket into the region in between the two sub domains (Fig. 6). This observation supports the notion that a change in side chain orientation of Trp288 accompanies the transformation of the protease core from open to closed conformation and vice versa, suggesting that the structural fluctuations contributing to the opening of the closed active conformation facilitate the re-orientation of Trp288.

Percentile of the Cys105-S and His262-Nδ ion pair

The separation between the catalytic triad residues Cys105 and His262 is a determining factor in whether or not the

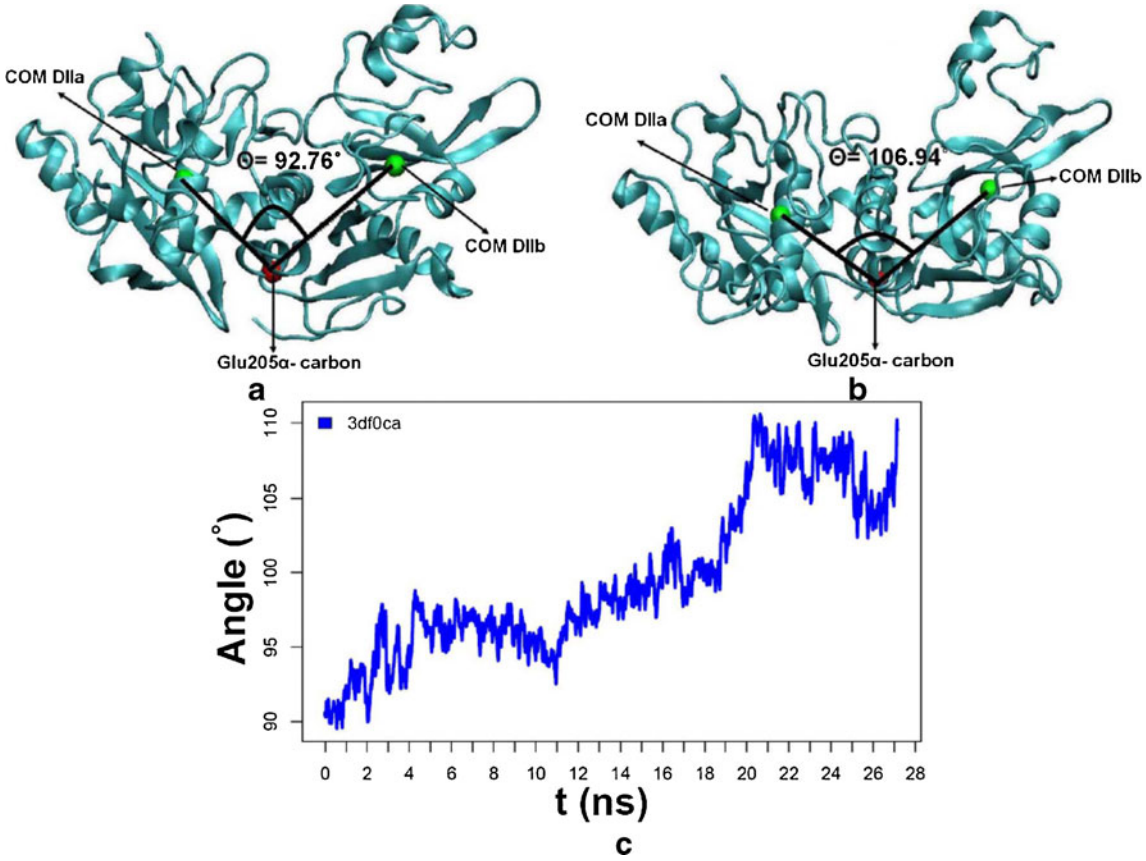

Fig. 5 Inter domain angle, Θ, of DIIa and DIIb of the protease core in model II (Ca^{2+}-bound protease core extracted from Ca^{2+}-bound m-calpain heterodimer, pdbid: 3df0) that exhibited Trp288 side chain rotation. **a** Snapshot showing Θ near the beginning of the simulation, Θ=92.76°. **b** Snapshot showing Θ near the end of the simulation, Θ= 106.94°. **c** Plot of Θ as a function of simulation time, *t*, for the same system. **a** and **b** were generated by using VMD [47]; **c** was generated by using R [51]

protease core of m-calpain is active. The distance between Cys105-S and His262-N_δ should be small enough for the S and N atoms to form an ion pair [21]. As mentioned before, we use an approximate distance of 4 Å as a criterion for the presence of a Cys105-S–His262-Nδ ion pair. A useful metric to discern if the protease core has a predisposition for the active conformation could be the proportion of time that the ion pair between Cys105-S and His262-Nδ is present in the protease core. Such a metric can hint at the likelihood of the system being active or inactive. For this reason, we calculated the proportion of time that Cys105-S and His262-N_δ are found within a 4 Å distance of each other. We refer to this conformation as the closed conformation.

Figure 7a presents the percentages of time that the catalytic residues Cys105/Ser105 and His262 form an ion pair (d<4 Å) when the distance is measured under different conditions. (Note that in the crystal structure of Ca^{2+}bound

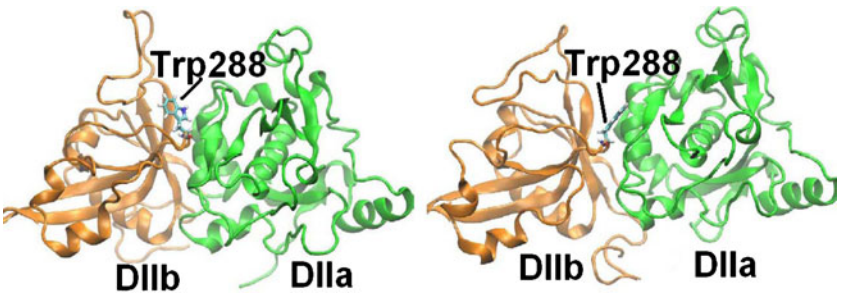

Fig. 6 Side chain orientation of Trp288 as observed by targeted molecular dynamics (TMD) simulation. **a** Original structure of protease core (closed and active conformation) before the application of constraints in the TMD simulation. **b** Structure of protease core towards the end of the TMD simulation. The figures were generated using VMD [50]

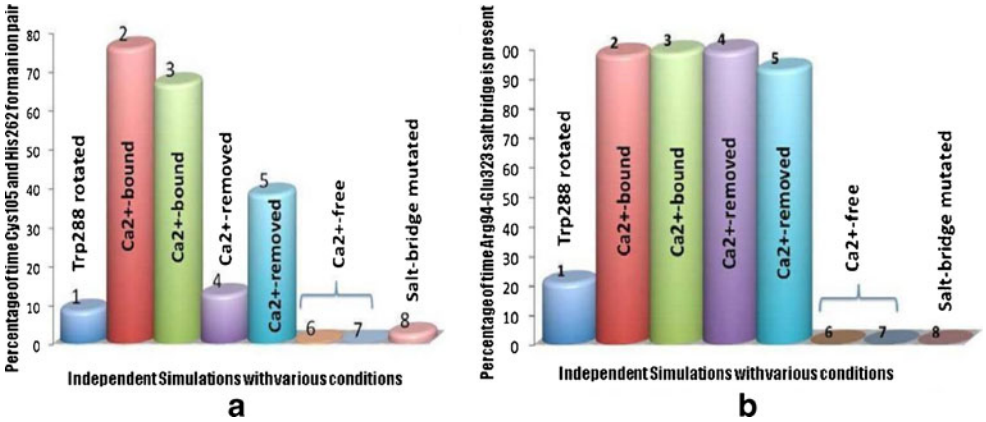

Fig. 7 Percentage of time that **a** the ion pair between Cys105-S and His262-Nδ is present and **b** the inter domain Arg94–Glu323 salt bridge remains intact. The plot shows the key factors affecting the active conformation. The numbers and labels represent different conditions: *1–3* independent simulations of model II; *4*, *5* independent simulations of model III; *6*, *7* independent simulations of model I, *8* represents the only simulation of model IV

m-calpain (pdbid: 3df0), Cys105 is mutated to Ser105 for crystallization and therefore the catalytic distance is calculated between Ser105-Oγ and His262-Nδ.) Similarly, Fig. 7b presents the percentages of time that the inter domain Arg94-Glu323 double salt bridge is present (d<4 Å) when the distances between the salt-bridge residues are measured under different conditions. In the figures, the numbers on the bars represent different independent simulations. The bars labelled 1–3 represent three independent simulations of Ca^{2+}-bound m-calpain protease core (model II). In one of these simulations (labelled 1), the side chain of Trp288 was observed to rotate from its closed conformation orientation. Otherwise, this is similar to the other two Ca^{2+}-bound protease cores labelled 2 and 3. Figure 7a reveals that the Ca^{2+}-bound protease core, with the reoriented Trp288 side chain, exhibits a smaller percentage of time in closed conformation as compared to the other two similar Ca^{2+}-bound structures. When examining the salt- bridge lifetime in Fig. 7b, the protease core with Trp288 reoriented (labelled 1) has a smaller percentage of time with intact salt-bridge structure. Note that, while the absence of salt-bridge affects significantly the lifetime of the protease core in the closed conformation, the mere presence of the salt-bridge does not fully guarantee an assembled catalytic triad. This can be seen from models 4 and 5, which show a relatively intact salt-bridge (Fig. 7b). In these models, the removal of Ca^{2+} has a significant influence on the stability of a closed conformation, resulting in a lower percentage time with Cys-His ion pair formation (cf. Fig. 7a). Generally, from Fig. 7a,b, all things being equal, Ca^{2+}-bound protease cores spend a higher percentage of time with an intact ion pair between catalytic residues Ser105 and His262 and therefore are much more likely to have an active conformation than the protease cores in the Ca^{2+}-removed condition.

Conclusion

We performed MD simulations of the protease core of m-calpain to assess the global and local conformational changes arising from calcium binding. We employed Ca^{2+}-free and Ca^{2+}-bound protease cores extracted from full size m-calpain crystal structures (pdbid: 1kfu and 3df0). Conventional MD simulations of the protease cores that are extracted from Ca^{2+}-free m-calpain heterodimer (model I; pdbid: 1kfu) revealed the importance of Ca^{2+}-binding in stabilizing the active conformation of the protease cores. Similar MD simulations of the protease cores extracted from Ca^{2+}-bound m-calpain heterodimer and simulated both in the presence (model II) and absence (model III) of calcium ions revealed that Ca^{2+}-bound protease cores are much more likely to retain the active conformation than Ca^{2+}-free protease cores.

Although Ca^{2+} was found to play role in establishing the active conformation of the protease core, other inter-related factors were also observed to affect the conformation and stability of protease cores. One important factor is the double salt-bridge between R94 and E323, which is present only in the protease core of Ca^{2+}-bound m- calpain. To examine the specific effect on the protease core of the disruption of the salt bridge, we performed E323A mutation in the protease core extracted from Ca^{2+}-bound m-calpain heterodimer (model IV) to manually break the salt bridge, then performed conventional MD simulations. The disruption of the salt-bridge increased the catalytic distance, d, from d=3.47 A to d~5 A, revealing a significant role for the inter domain salt-bridge in maintaining the closed, catalytically competent conformation. Another Ca^{2+}-dependent factor reported to play a role in determining the conformation of the protease core of m-calpain is the side chain orientation of Trp288. In one of the conventional MD simulations

of model II (protease core of calcium bound m- calpain), we observed a transformation of the Ca^{2+}-bound protease core from closed to open conformation when assessed in terms of both the catalytic distance, *d*, and inter domain angle, Θ. In the same simulation, the side chain of Trp288 moved away from the hydrophobic pocket located in IIb, into the region between the two sub domains, IIa and IIb, exhibiting correlation between the tryptophan orientation and interdomain conformation. This observation prompted us to use targeted molecular dynamics (TMD) simulations that can capture such a transition by overcoming the potential barrier against the free rotation of Trp288 side chain. The TMD simulation affirmed that the Trp288 undergoes sidearm orientations similar to those observed in the crystal structures of the protease core as the two lobes of the core changes from closed to open conformation.

In conclusion, the present study affirmed the role of factors such as the Arg94–Glu323 salt bridge, Trp288 reorientation and Ca^{2+}-binding in the formation and stabilization of the catalytically competent active conformation. Using the catalytic distance, *d*, as a metric, we observed that deletion of the salt bridge through mutation destabilizes formation of the catalytically competent conformation, even in the Ca^{2+}-bound situation (cf. Fig. 7a). This suggests that the Arg94-Glu323 double salt-bridge is important in stabilization of the catalytically competent conformation. In the unmutated structures, although not as much as the deletion of the salt-bridges (compare 4, 5 and 8 in Fig. 7a), the removal of Ca^{2+} is observed to affect the stability of the catalytically competent conformation. In general, once the protease core adopts a catalytically competent conformation, each of the above mentioned factors becomes indispensable, acting together to stabilize the closed active conformation.

Finally, it should be pointed out that the present study focused on the protease core in a manner similar to the experimental studies that investigated mini-calpains. In the real system, although tension from neighboring domains is released upon calcium binding and activation, these domains may still have an influence on the stability and conformation of the protease core. To fully understand the effect of neighboring domains, a similar study of full-size m-calpain would be necessary, and our future work will address these issues.

References

1. Ono Y, Sorimachi H, Suzuki K (1998) Structure and physiology of calpain, an enigmatic protease. Biochem Biophys Res Commun 245(2):289–294
2. Carafoli E, Molinari M (1998) Calpain: a protease in search of a function? Biochem Biophys Res Commun 247(2):193–203
3. Ohno S, Emori Y, Imajoh S, Kawasaki H, Kisaragi M, Suzuki K (1984) Evolutionary origin of a calcium-dependent protease by fusion of genes for a thiol protease and a calcium-binding protein? Nature 312(5994):566–570
4. Sorimachi H, Ishiura S, Suzuki K (1997) Structure and physiological function of calpains. Biochem J 328:721–732
5. Suzuki K, Sorimachi H (1998) A novel aspect of calpain activation. FEBS Lett 433(1–2):1–4
6. Goll DE, Thompson VF, Li H, Wei W, Cong J (2003) The calpain system. Physiol Rev 83(3):731–801
7. Grynspan F, Griffin WB, Mohan PS, Shea TB, Nixon RA (1997) Calpains and calpastatin in SH-SY5Y neuroblastoma cells during retinoic acid-induced differentiation and neurite outgrowth: comparison with the human brain calpain system. J Neurosci Res 48(3):181–191
8. Song DK, Malmstrom T, Kater SB, Mykles DL (1994) Calpain inhibitors block ca(2+)-induced suppression of neurite outgrowth in isolated hippocampal pyramidal neurons. J Neurosci Res 39 (4):474–481
9. Tomimatsu Y, Idemoto S, Moriguchi S, Watanabe S, Nakanishi H (2002) Proteases involved in long-term potentiation. Life Sci 72 (4–5):355–361
10. Huang Y, Wang KK (2001) The calpain family and human disease. Trends Mol Med 7(8):355–362
11. McCracken E, Hunter AJ, Patel S, Graham DI, Dewar D (1999) Calpain activation and cytoskeletal protein breakdown in the corpus callosum of head-injured patients. J Neurotrauma 16(9):749–761
12. Buki A, Siman R, Trojanowski JQ, Povlishock JT (1999) The role of calpain-mediated spectrin proteolysis in traumatically induced axonal injury. J Neuropathol Exp Neurol 58(4):365–375
13. Gennarelli TA, Thibault LE, Adams JH, Graham DI, Thompson CJ, Marcincin RP (1982) Diffuse axonal injury and traumatic coma in the primate. Ann Neurol 12(6):564–574
14. Friedrich P (2004) The intriguing Ca^{2+} requirement of calpain activation. Biochem Biophys Res Commun 323(4):1131–1133
15. Strobl S, Fernandez-Catalan C, Braun M et al (2000) The crystal structure of calcium-free human m-calpain suggests an electrostatic switch mechanism for activation by calcium. Proc Natl Acad Sci USA 97(2):588–592
16. Hosfield CM, Elce JS, Davies PL, Jia Z (1999) Crystal structure of calpain reveals the structural basis for Ca^{2+}-dependent protease activity and a novel mode of enzyme activation. EMBO J 18 (24):6880–6889
17. Suzuki K, Hata S, Kawabata Y, Sorimachi H (2004) Structure, activation, and biology of calpain. Diabetes 53(Suppl 1):12–18
18. Chou JS, Impens F, Gevaert K, Davies PL (2011) m-calpain activation in vitro does not require autolysis or subunit dissociation. Biochim Biophys Acta 1814(7):864–872
19. Alvarez J, Montero M, Garcia-Sancho J (1999) Subcellular $Ca^{(2+)}$ dynamics. News Physiol Sci 14:161–168
20. Moldoveanu T, Hosfield CM, Lim D, Jia Z, Davies PL (2003) Calpain silencing by a reversible intrinsic mechanism. Nat Struct Biol 10(5):371–378
21. Moldoveanu T, Hosfield CM, Lim D, Elce JS, Jia Z, Davies PL (2002) A $ca^{(2+)}$ switch aligns the active site of calpain. Cell 108 (5):649–660
22. Davis TL, Walker JR, Finerty PJ, Mackenzie F, Newman EM, Dhe-Paganon S (2007) The crystal structures of human calpains 1 and 9 imply diverse mechanisms of action and auto-inhibition. J Mol Biol 366(1):216–229
23. Moldoveanu T, Gehring K, Green DR (2008) Concerted multi-pronged attack by calpastatin to occlude the catalytic cleft of heterodimeric calpains. Nature 456(7220):404–408
24. Reverter D, Strobl S, Fernandez-Catalan C, Sorimachi H, Suzuki K, Bode W (2001) Structural basis for possible calcium-induced activation mechanisms of calpains. Biol Chem 382(5):753–766
25. Kamphuis IG, Kalk KH, Swarte MB, Drenth J (1984) Structure of papain refined at 1.65 A resolution. J Mol Biol 179(2):233–256

26. Lewis SD, Johnson FA, Shafer JA (1976) Potentiometric determination of ionizations at the active site of papain. Biochemistry 15 (23):5009–5017
27. Shesham RD, Bartolotti LJ, Li Y (2008) Molecular dynamics simulation studies on Ca^{2+} -induced conformational changes of annexin I. Protein Eng Des Sel 21(2):115–120
28. Li J, Geng C, Bu Y, Huang X, Sun C (2009) Conformational transition pathway in the allosteric process of calcium-induced recoverin: molecular dynamics simulations. J Comput Chem 30 (7):1135–1145
29. Komeiji Y, Ueno Y, Uebayasi M (2002) Molecular dynamics simulations revealed Ca^{2+}-dependent conformational change of calmodulin. FEBS Lett 521(1–3):133–139
30. Shepherd CM, Vogel HJ (2004) A molecular dynamics study of Ca^{2+}-calmodulin: Evidence of interdomain coupling and structural collapse on the nanosecond timescale. Biophys J 87(2):780–791
31. Project E, Friedman R, Nachliel E, Gutman M (2006) A molecular dynamics study of the effect of Ca^{2+} removal on calmodulin structure. Biophys J 90(11):3842–3850
32. Barlow DJ, Thornton JM (1983) Ion-pairs in proteins. J Mol Biol 168(4):867–885
33. Kumar S, Nussinov R (1999) Salt bridge stability in monomeric proteins. J Mol Biol 293(5):1241–1255
34. Kumar S, Ma B, Tsai CJ, Nussinov R (2000) Electrostatic strengths of salt bridges in thermophilic and mesophilic glutamate dehydrogenase monomers. Proteins 38(4):368–383
35. Moldoveanu T, Jia Z, Davies PL (2004) Calpain activation by cooperative Ca^{2+} binding at two non-EF-hand sites. J Biol Chem 279(7):6106–6114
36. Brooks BR, Bruccoleri RE, Olafson BD, States DJ, Swaminathan S, Karplus M (1983) CHARMM: a program for macromolecular energy, minimization, and dynamics calculations. J Comput Chem 4(2):187–217
37. Jorgensen WL, Chandrasekhar J, Madura JD (1983) Comparison of simple potential functions for simulating liquid water. J Chem Phys 79(2):926
38. Grubmüller H (1996) Solvate: a program to create atomic solvent models, ver 1.0. Theoretical Biophysics Group, Institut für Medizinische Optik, Ludwig-Maximilians-Universität München, Munich, Germany
39. Phillips JC, Braun R, Wang W et al (2005) Scalable molecular dynamics with NAMD. J Comput Chem 26(16):1781–1802
40. MacKerell AD, Bashford D, Bellott et al (1998) All-atom empirical potential for molecular modeling and dynamics studies of proteins. J Phys Chem B 102(18):3586–3616
41. Darden T, York D, Pedersen L (1993) Particle mesh ewald: An N·log(N) method for Ewald sums in large systems. J Cheml Phys 98(12):10089
42. Chu JW, Voth GA (2005) Allostery of actin filaments: molecular dynamics simulations and coarse-grained analysis. Proc Natl Acad Sci USA 102(37):13111–13116
43. Lee HS, Robinson RC, Joo CH, Lee H, Kim YK, Choe H (2006) Targeted molecular dynamics simulation studies of calcium binding and conformational change in the C-terminal half of gelsolin. Biochem Biophys Res Commun 342(3):702–709
44. Perdih A, Kotnik M, Hodoscek M, Solmajer T (2007) Targeted molecular dynamics simulation studies of binding and conformational changes in *E. coli* MurD. Proteins 68(1):243–254
45. Provasi D, Murcia M, Coller BS, Filizola M (2009) Targeted molecular dynamics reveals overall common conformational changes upon hybrid domain swing-out in beta3 integrins. Proteins 77(2):477–489
46. Schlitter J, Engels M, Krüger P (1994) Targeted molecular dynamics: A new approach for searching pathways of conformational transitions. J Mol Graph 12(2):84–89
47. Schlitter J, Engels M, Krüger P, Jacoby E, Wollmer A (1993) Targeted molecular dynamics simulation of conformational change-application to the T ↔ R transition in insulin. Mol Simul 10(2–6):291–308
48. Im W, Lee MS, Brooks CL (2003) Generalized born model with a simple smoothing function. J Comput Chem 24(14):1691–1702
49. Chen J, Im W, Brooks CL (2006) Balancing solvation and intramolecular interactions: toward a consistent generalized born force field. J Am Chem Soc 128(11):3728–3736
50. Humphrey W, Dalke A, Schulten K (1996) VMD: Visual molecular dynamics. J Mol Graph 14(1):33–38
51. R Development Core Team (2011) R: a language and environment for statistical computing. R Foundation for Statistical Computing, Vienna, Austria. ISBN 3-900051-07-0